THE PUBLISHING HOUSE
OF THE ROMANIAN ACADEMY

PROCEEDINGS OF THE ROMANIAN ACADEMY, Series A,
Volume 7, Number 3/2006, pp. 000-000

THIN HYDROFOIL CASCADE DESIGN AND NUMERICAL FLOW ANALYSIS PART II - ANALYSIS

Romeo SUSAN-RESIGA[†‡], Sebastian MUNTEAN[‡], Sandor BERNAD[‡], Teodora FRUNZĂ[†], Daniel BALINT[†]

[†] "Politehnica" University of Timişoara, Bd. Mihai Viteazu 1, RO-300222, Timişoara
[‡] Romanian Academy - Timişoara Branch, Center for Advanced Research in Engineering Sciences, Bd. Mihai Viteazu 24, RO-300222, Timişoara
Corresponding author: Romeo SUSAN-RESIGA, "Politehnica" University of Timişoara, Bd. Mihai Viteazu 1, RO-300222, Timişoara, phone: ++40-256-403692; fax: ++40-256-403700, e-mail: resiga@mh.mec.upt.ro

The two-part paper presents the development and implementation of robust, efficient and accurate numerical algorithms for hydrofoil cascade design, analysis and optimization. In this second part we analyze in the incompressible, inviscid and irrotational flow in thin hydrofoil turbine cascades using two numerical methods. We briefly present our Finite Element methodology for analyzing cascade flows with streamfunction formulation. We evaluate the accuracy of our CASCADExpert code for two thin hydrofoil cascades designed with the quasi-analytical approach. Then, the same test cases are analyzed with the Finite Volume approach for the primary variables formulation using the commercial code FLUENT. The numerical accuracy is again assessed in comparison with quasi-analytical test cases, and the numerical mechanism that replaces the Kutta-Joukowsky condition is revealed. Both numerical methods investigated in this paper are shown to be robust and accurate, thus providing a valuable set of numerical tools for design, analysis and optimization of hydrofoil cascades, to be used in modern hydraulic turbomachinery design and optimization.

Keywords: Thin hydrofoil cascade, Finite Element Method, Finite Volume Method.

1. INTRODUCTION

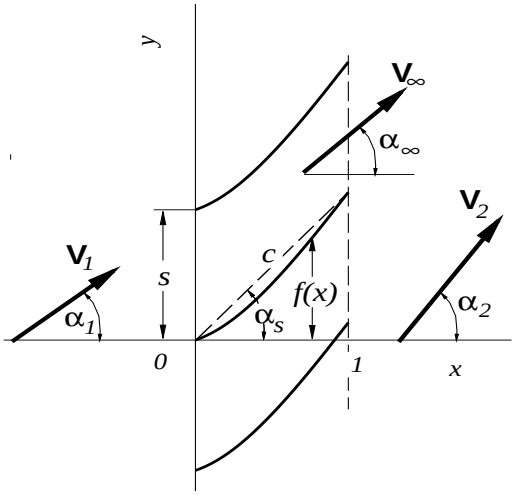

Fig. 1. Thin hydrofoil cascade notations.

In the first part of this paper [15] we have presented the quasi-analytical method for designing thin hydrofoil cascades, based on the non-linear integral equation given by Hawthorne et al. [8], and an iterative algorithm which uses a piecewise cubic, with continuous derivatives, of the thin blade shape. Two thin blade turbine cascades have been designed, and are used as reference cases within this paper to assess the accuracy and robustness of both Finite Element and Finite Volume numerical methods for analyzing the flow field.

The notations employed in this paper are shown in Fig.1. The starting point for the thin hydrofoil cascade design is the schedule of the pitch-averaged velocity,

$$\overline{\mathbf{V}}(x)=\frac{1}{s}\int_0^s \mathbf{V}(x,y)\,\mathrm{d}y\,. \qquad (1)$$

Since the pitch-wise averaged meridional component of the velocity, $\overline{V}_x$, is constant for blades with vanishing thickness, we actually prescribe the schedule of the pitch-wise averaged tangential velocity,

Recommended by Ioan ANTON, member of the Romanian Academy

$$\overline{V}_y(x)=\overline{V}_{y1}+\int_0^x\overline{\gamma}(t)\mathrm{d}t\text{, where }\overline{\gamma}(x)\equiv\frac{\gamma(x)}{s}=\frac{\mathrm{d}\overline{V}_y}{\mathrm{d}x}. \tag{2}$$

With the pressure coefficient defined with respect to the upstream conditions, using Eqs. 16…19 from [15] one can easily show that the pressure jump from the pressure side to the suction side of the thin foil can be written as

$$\Delta c_p(x)=2s\overline{\gamma}(x)\frac{V_{x\mathrm{bl}}(x)}{\overline{V}_x}\cos^2\alpha_1, \tag{3}$$

where $V_{x\mathrm{bl}}(x)$ is the meridional component of the average tangential velocity on the blade, and $\overline{\gamma}(x)$ is the pitchwise averaged boundary velocity. Eq. (3) clearly shows that $\overline{\gamma}(x)$ is directly related to the blade loading distribution $\Delta c_p(x)$. Two turbine cascades have been designed in [15] for a vortex strength distribution $\overline{\gamma}(x)=(\tan\alpha_2-\tan\alpha_1)\sqrt{x}(1-x)15/4$ and two spacing values, $s=1$ and $s=2$, respectively. Both cascades have the upstream flow angle $\alpha_1=35^\circ$ and downstream flow angle $\alpha_2=55^\circ$. These benchmark cases are used as reference in this paper to assess the accuracy of flow field numerical solutions.

The present paper presents the authors ongoing efforts to develop a robust and efficient numerical methodology, and the associated expert software, for analysis, design and optimization of hydrofoil cascades. The main goal is to automatically optimize the hydrofoil shape for best efficiency as well as for best cavitational characteristics. So far, we have developed a Finite Element solver for incompressible, inviscid and irrotational cascade flow [14], using a modern software infrastructure [1], and efficient implementation of boundary conditions [12] or solution postprocessing techniques [7]. Numerical results were validated with experimental data [2], [13] or with other numerical results. In this paper we present a more difficult test case corresponding to the thin hydrofoil cascade, where the robustness of our Kutta-Joukowski condition implementation is verified. By using the latest implementation techniques and efficient iterative solvers for large sparse systems of linear equations, we achieve the same performances as methods based on integral equation solution [10], with the additional benefit of obtaining the hydrodynamic field in the whole computational domain and not only on the blade surface.

Section 2 summarizes the mathematical and numerical foundation of our computer code CASCADExpert, and assesses the accuracy of our code for the two test cases designed in the first part of this paper [15]. Section 3 solves the two turbine cascades using the FLUENT expert code, and reveals the numerical mechanism which replaces the explicit Kutta-Joukowsky condition when a primary variable Euler solver is employed. The paper conclusions are summarized in Section 4.

2. THIN HYDROFOIL CASCADE ANALYSIS USING FINITE ELEMENT METHOD FOR STREAMFUNCTION FORMULATION

The inviscid, incompressible and irrotational flow model employed by our software CASCADExpert is based on the streamfunction formulation [14]. For incompressible flows the divergence of the velocity vanishes everywhere. Vectors satisfying this condition are called solenoidal (or divergence free), i.e. $\nabla\cdot\mathbf{V}=0$. Any solenoidal vector can be written as the curl of another vector, called the vector potential, $\mathbf{V}=\nabla\times\boldsymbol{\beta}$. For 2D plane flow, the vector potential is $\boldsymbol{\beta}=\psi\mathbf{e}_z$, where $\mathbf{e}_z$ is the unit vector in the direction normal to the plane of flow. The velocity components in the x- and y-directions are

$$V_x(x,y)=\frac{\partial\psi(x,y)}{\partial y}\text{ and }V_y(x,y)=-\frac{\partial\psi(x,y)}{\partial x} \tag{4}$$

Since the gradient of ψ is normal to the velocity vector, along a streamline we have $\psi=\text{constant}$, thus the name *streamfunction*. A flow that is both irrotational and incompressible must satisfy both the conditions of

zero curl $\nabla \times \mathbf{V} = \mathbf{0}$ and zero divergence. The second is automatically satisfied by introducing the streamfunction (5), and enforcing the irrotationality condition leads to the 2D Laplace equation

$$\frac{\partial^2 \psi(x,y)}{\partial x^2} + \frac{\partial^2 \psi(x,y)}{\partial y^2} = 0 \tag{5}$$

In order to define the boundary value problem for ψ we introduce the appropriate cascade boundary conditions. First, the computational domain is chosen as a periodic strip, resulting in a double connected domain as in Fig. 2, with the following boundary segments:

- Fluid boundary (inlet, outlet, periodic); the periodic boundary segments are obtained by translation with the cascade pitch in the direction of the cascade frontline; the inlet/outlet boundaries are aligned with the cascade front line. Note that the shape of the periodic boundary segments is arbitrary, the only constraint being the constant width of the strip.
- Solid boundary (hydrofoil surface), with a unit-length chordline and stagger angle α_s. In order to perform a numerical analysis of the thin hydrofoil, a small thickness of $O\left(10^{-3}\right)$ is added to discriminate between the nodes on the upper and lower side of the foil.

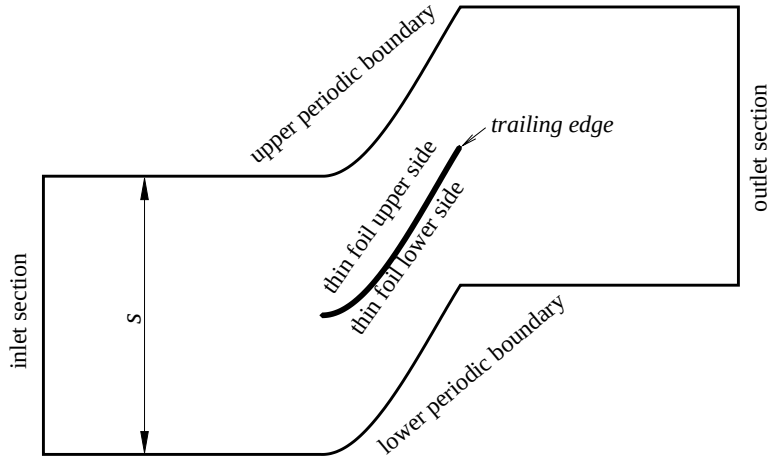

Fig. 2. Double-connected computational domain for finite element analysis.

In specifying the following boundary conditions we consider a unit axial velocity component upstream and downstream the cascade, and a unit chord length. As a result, the cascade pitch is made dimensionless by the hydrofoil chord, i.e. we use s/c, while in the previous section the unit length has been chosen the axial extent of the cascade. Obviously, in design problems we cannot use the chord as reference length since neither the hydrofoil, nor the stagger angle, are known apriori.

On each boundary point only one condition can be specified since we have only one unknown function. On the inlet section, only the tangential velocity component is specified as

$$\frac{\partial \psi}{\partial n} = \tan\alpha_1 \text{ on inlet.} \tag{6}$$

On the outlet section we are using the same type of condition, but in this case the flow direction is not known apriori. As a result we have

$$\frac{\partial \psi}{\partial n} + \tan\alpha_2 = 0 \text{ on outlet,} \tag{7}$$

where the outflow direction $\tan\alpha_2$ is an additional unknown of the problem. For a pair of points from the upper and lower periodic boundaries, having the same abscissa, the velocity vector must be the same. The

periodicity of the velocity tangent to the periodic boundary leads to the following periodic Neumann condition,

$$\left(\frac{\partial\psi}{\partial n}\right)_{up}+\left(\frac{\partial\psi}{\partial n}\right)_{lo}=0 \text{ on periodic boundary.} \tag{8a}$$

On the other hand, since on inlet/outlet sections we have specified only the direction of the flow, we must prescribe the flowrate as well. This can be done via the Dirichlet-type condition for any pair of points on the periodic boundaries,

$$\psi_{up}-\psi_{lo}=\frac{s}{c} \text{ on periodic boundary.} \tag{8b}$$

Condition (8b) also implies the periodicity of the velocity normal to the periodic boundaries, i.e.

$$\left(\frac{\partial\psi}{\partial\tau}\right)_{up}+\left(\frac{\partial\psi}{\partial\tau}\right)_{lo}=0 \text{ on periodic boundary.}$$

On the hydrofoil surface the inviscid flow condition corresponds to vanishing normal velocity. In other words the hydrofoil is a streamline, and without loosing generality we can set

$$\psi=0 \text{ on hydrofoil.} \tag{9}$$

In order to close the problem we need an additional condition for the unknown flow direction downstream $\tan\alpha_2$. This condition is derived from Joukowsky's hypothesis [11, §7.40]: the circulation in the case of a properly designed aerofoil always adjusts itself so that the velocity at the trailing edge is finite. This condition appears to be satisfied with reasonable exactness within the working range of well designed aerofoils. Within the present formulation the Joukowski's condition is implemented by formally setting the trailing edge to be a stagnation point,

$$\frac{\partial\psi}{\partial n}=0 \text{ at the trailing edge.} \tag{10}$$

It is obvious that (10) has no meaning for sharp trailing edges, or for foils with zero thickness. However, within the weak formulation of the finite element the actual implementation of (10) agrees with the physical considerations leading to the Joukowsky's condition.

The problem (5), with conditions (6…10) is well defined and allows the computation of the streamfunction as well as the direction of the flow downstream the cascade. Once the streamfunction known, the velocity field can be recovered using (4), and the pressure field follows from the Bernoulli's theorem. The elliptic boundary value problem for the streamfunction is solved with the Finite Element Method [9] using our CASCADExpert code [6].

The starting point in the Finite Element Method is the variational formulation. We introduce the following functional,

$$F(\psi)=\frac{1}{2}\iint_{\Omega}\left[\left(\frac{\partial\psi}{\partial x}\right)^2+\left(\frac{\partial\psi}{\partial y}\right)^2\right]\mathrm{d}x\,\mathrm{d}y-\int_{\Gamma_N}\psi\,f_N\,\mathrm{d}\Gamma, \tag{11}$$

where Ω denotes the two-dimensional computational domain, and Γ_N is the part of the domain boundary where Neumann conditions are imposed, with Neumann data $\partial\psi/\partial n=f_N$. The solution of the original boundary value problem (5…10) will be the one that corresponds to the extremum of functional (11) while satisfying the Dirichlet conditions. Note that by using this approach we have only first order partial derivatives instead of second order ones in the original Laplace equation (5).

The computational domain is discretized with triangular elements, resulting in an unstructured mesh. Then, the streamfunction is approximated using its nodal values ψ_j and the finite element shape functions $N_j(x,y)$, as follows:

$$\psi(x,y) \cong \sum_j \psi_j N_j(x,y). \tag{12}$$

Introducing the finite element approximation (12) in (11) transforms the functional into a function depending on the streamfunction nodal values,

$$F(\psi_1,\psi_2,\ldots) = \frac{1}{2}\iint_\Omega \left[\left(\sum_j \psi_j \frac{\partial N_j}{\partial x} \right)^2 + \left(\sum_j \psi_j \frac{\partial N_j}{\partial y} \right)^2 \right] \mathrm{d}x\,\mathrm{d}y - \int_{\Gamma_N} \left(\sum_j \psi_j N_j \right) f_N \,\mathrm{d}\Gamma . \tag{13}$$

The extremum of the above function is found by cancelling all partial derivatives with respect to the nodal values, leading to the following system of equations:

$$\frac{\partial F}{\partial \psi_i} = \sum_j \psi_j \iint_\Omega \left[\frac{\partial N_i}{\partial x}\frac{\partial N_j}{\partial x} + \frac{\partial N_i}{\partial y}\frac{\partial N_j}{\partial y} \right] \mathrm{d}x\,\mathrm{d}y - \int_{\Gamma_N} N_i f_N \,\mathrm{d}\Gamma = 0 . \tag{14}$$

The main advantage in using FEM is found in the implementation of Neumann conditions. For example, at the trailing edge where both impenetrability and the Joukowski conditions must be imposed we have the following two equations in the system

$$\psi_{TE} = 0 \text{, impenetrability condition (9),}$$

$$\sum_j \psi_j \iint_\Omega \left[\frac{\partial N_{TE}}{\partial x}\frac{\partial N_j}{\partial x} + \frac{\partial N_{TE}}{\partial y}\frac{\partial N_j}{\partial y} \right] \mathrm{d}x\,\mathrm{d}y = 0 \text{, Joukowski's condition (10).} \tag{15}$$

We immediately note that there is no need to actually compute the normal derivative at the sharp trailing edge. In fact, instead of cancelling the normal derivative point-wise as would be required by (10), we are cancelling the local flux. The periodic Neumann condition (8a) is simply implemented by adding up two rows from the assembled matrix [12]. Once again, there is no need to evaluate the normal derivative, which is an important advantage in terms of accuracy (especially on unstructured meshes) and robustness:

$$\sum_j \psi_j \iint_\Omega \left[\frac{\partial N_{up}}{\partial x}\frac{\partial N_j}{\partial x} + \frac{\partial N_{up}}{\partial y}\frac{\partial N_j}{\partial y} \right] \mathrm{d}x\,\mathrm{d}y + \sum_j \psi_j \iint_\Omega \left[\frac{\partial N_{lo}}{\partial x}\frac{\partial N_j}{\partial x} + \frac{\partial N_{lo}}{\partial y}\frac{\partial N_j}{\partial y} \right] \mathrm{d}x\,\mathrm{d}y = 0 . \tag{16}$$

The actual implementation [5,6] of our finite element solver CASCADExpert is done using the Portable Extensible Toolkit for Scientific Computation (PETSc) [1]. The linear system of equations, with sparse matrix, is solved iteratively using the preconditioned BiConjugate Gradient Method, with Incomplete LU factorization as preconditioner.

Once the nodal values for the streamfunction found, the velocity on the hydrofoil can be computed using the same weak form for the normal derivative.

$$V_\tau = -\frac{\partial \psi}{\partial n}, \text{ or the weak form } V_\tau \Delta s = -\sum_j \psi_j \iint_\Omega \left[\frac{\partial N_F}{\partial x}\frac{\partial N_j}{\partial x} + \frac{\partial N_F}{\partial y}\frac{\partial N_j}{\partial y} \right] \mathrm{d}x\,\mathrm{d}y , \tag{17}$$

where F denotes a point on the foil where the velocity V_τ is computed, and Δs is the average length of two boundary segments adjacent to the node F. Note that the right-hand side in (17) is readily obtained by assembling the finite element matrices into the global matrix. The global matrix rows are saved before altering them for implementing the Dirichlet condition (9), then used in the post-processing step. The right-hand side of (17) is simply computed by multiplying the saved matrix rows with the solution vector.

In conclusion, using the variational formulation of the original boundary value problem within the finite element framework offers essential advantages for implementing the boundary conditions as well as for computing the velocity on the hydrofoil surface.

Let us examine the two turbine cascades designed in the first part of this paper [15]. Since the CASCADExpert code solves the boundary value problem for the streamfunction, we can directly plot the streamline pattern. Figures 3.a) and 3.b) show the streamlines for a periodic strip. One can easily observe the "shock-free" inlet on the blade corresponding to the continuous slope of the streamline $\psi = 0$ that passes

through the origin. This streamline includes the thin blade, and it can be seen the rather large curvature just upstream the blade leading edge (coordinate origin) that aligns the velocity vector to the camberline tangent direction. Once again, we emphasize that the "shock-free" condition is not at all met by simply aligning the far upstream flow with the camberline at leading edge. This would be the case only for an infinite number of blades in the limit $s \to 0$, which is only a theoretical asympthotic hypothesis.

Once the streamfunction computed, the velocity on the blade is computed using (17). Then, the pressure coefficient is evaluated with respect to the upstream conditions. The exact solution computed in [15] is compared with the FEM solution obtained with our code CASCADExpert in Figures 3.c) and 3.d). The agreement is very good, proving not only the accuracy of the streamfunction solution but also the accuracy of the normal derivative computation (17) required for the tangential velocity on the blade. Although the implementation Kutta-Joukowsky condition (10) leads to the correct overall flow deflection, as well as to the correct pressure distribution on the blade, a few points in the neighborhood of the trailing edge display a small velocity dispersion in comparison with the exact solution. It is not yet clear if this numerical problem is caused by the accuracy of the streamfunction computation in the trailing edge neighborhood or by the evaluation of the normal derivative. However, this minor numerical problem does not alter the overall accuracy of the FEM solution.

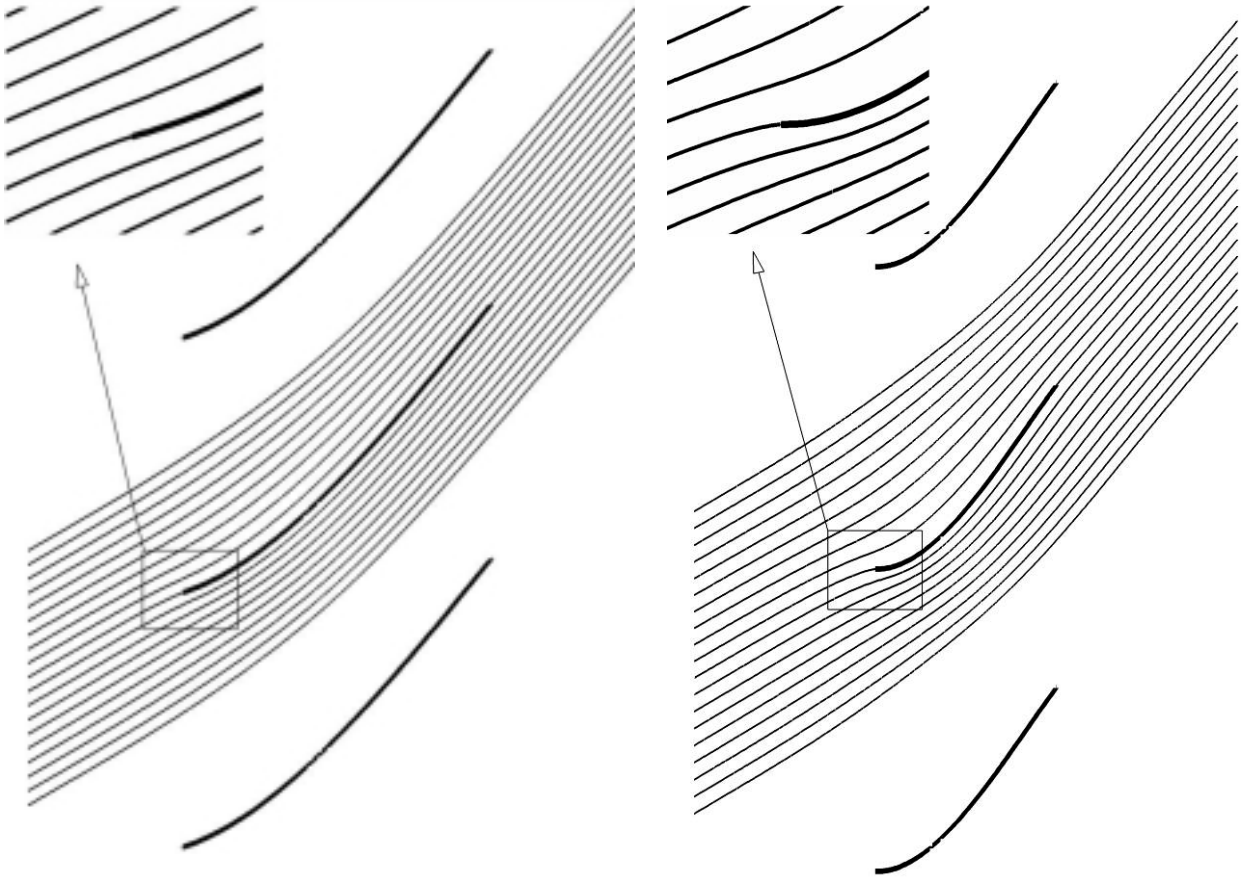

a) Streamlines for $s/c = 0.6614532$.

b) Streamlines for $s/c = 1.270120$.

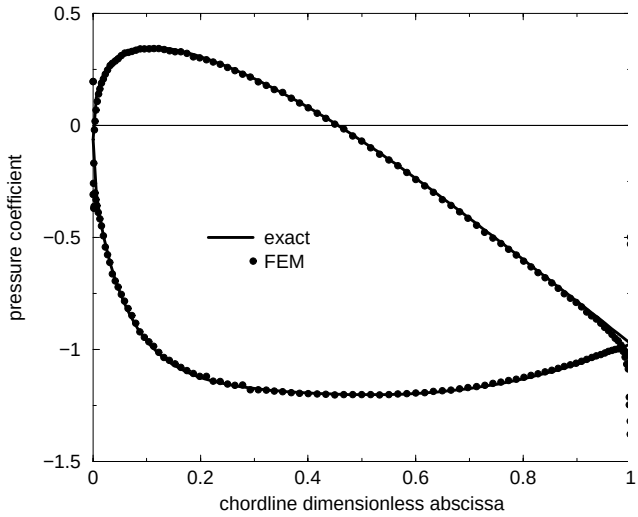

c) Pressure coefficient for $s/c = 0.6614532$.

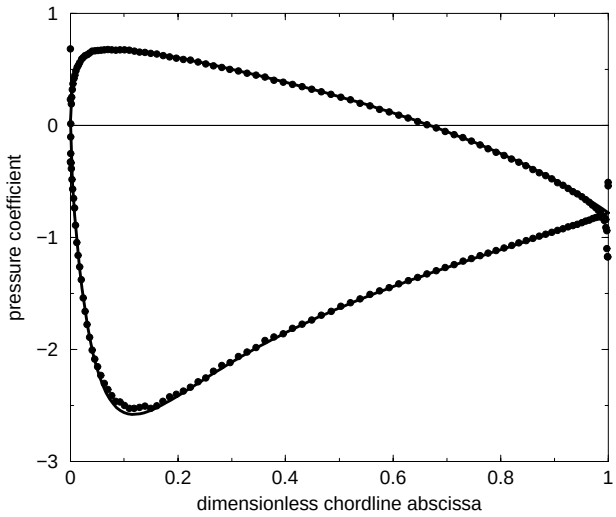

b) Pressure coefficient for $s/c = 1.270120$.

Figure 3. Streamlines and pressure coefficient for turbine cascade with $\alpha_1 = 35^\circ$ and $\alpha_2 = 55^\circ$ and two pitch/chord ratio values. Streamlines are computed with FEM. Pressure coefficient is computed both analytically (solid line) and numerically from FEM solution (dots).

3. THIN HYDROFOIL CASCADE ANALYSIS USING FINITE VOLUME METHOD FOR EULER EQUATIONS

The cascade flow can be analyzed using the primary variables formulation, i.e. by solving the Euler equations for incompressible steady flow,

$$\nabla \cdot \mathbf{V} = 0 \text{ , continuity equation,} \tag{18a}$$

$$(\mathbf{V} \cdot \nabla)\mathbf{V} = -\frac{1}{\rho}\nabla p \text{ , momentum equation.} \tag{18b}$$

In this paper we are using the Finite Volume Method solver from the FLUENT [16] commercial software. The computational domain is chosen single connected, as shown in Fig. 4, and a mesh of quadrilateral cells is generated with the GAMBIT pre-processor.

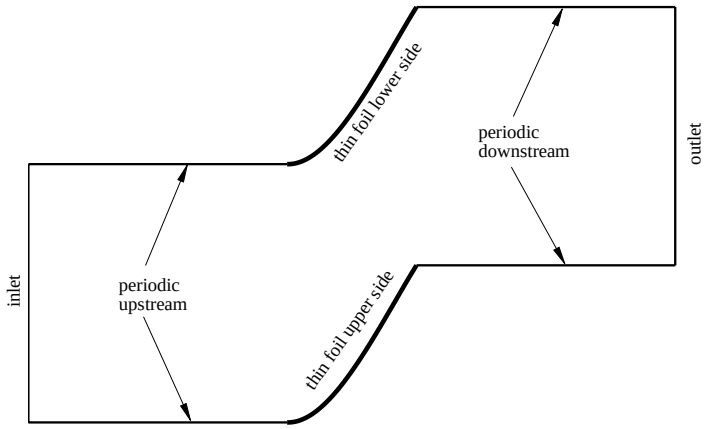

Figure 4. Computational domain for finite volume analysis.

The boundary conditions for the primary variable formulation are as follows:

- On inlet we specify the axial, $\bar{V}_x$, and tangential, $\bar{V}_{y1}$, velocity components;

- On outlet we impose a constant pressure condition;
- On the thin hydrofoil the normal velocity component vanishes;
- Velocity and pressure periodicity is enforced on the upstream and downstream periodic boundary segments.

Note that the Kutta-Joukowsky condition is missing from the above problem setup. Since an inviscid flow is assumed, one may ask why the pressure on the upper and lower sides of the thin hydrofoil would reach the same value as we approach the trailing edge from both sides?

Let us examine first the numerical results obtained with the FLUENT Finite Volume code for the two turbine cascades from [15]. The pressure distributions on the blade, shown in Figures 5 and 6, are in good agreement with the exact solution, with a small underestimation of the pressure magnitude on the suction side close to the leading edge. However, the thin blade design procedure for a shock-free flow is once again confirmed by the numerical results. For completeness we also present in Figures 5 and 6 the more qualitative pressure distribution in the computational domain.

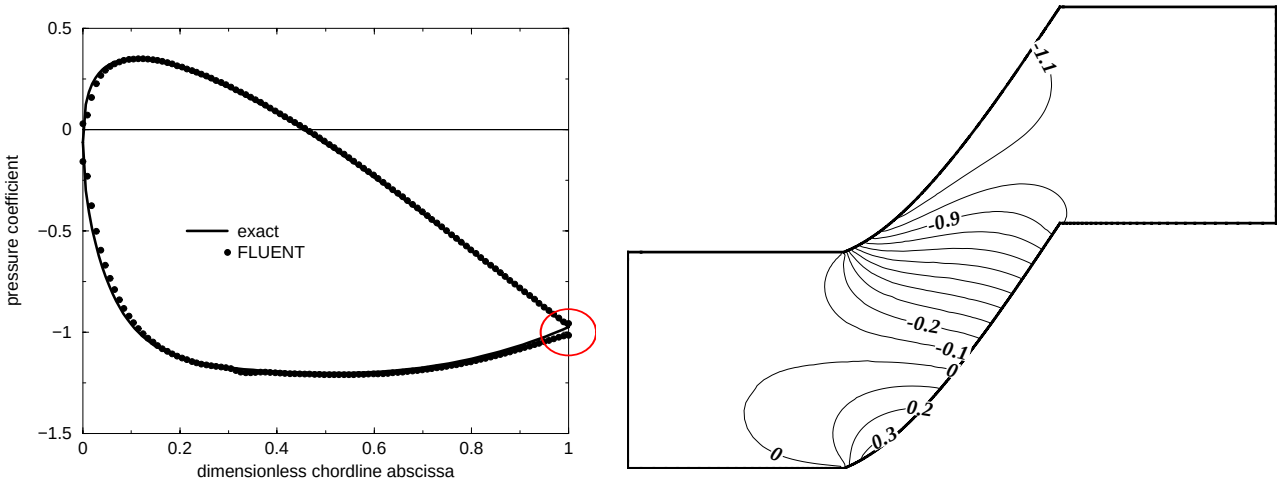

Figure 5. Pressure coefficient computed with FLUENT on the blade and in the inter-blade channel for a turbine cascade with $\alpha_1 = 35^\circ$ and $\alpha_2 = 55^\circ$ and $s/c = 0.6614532$.

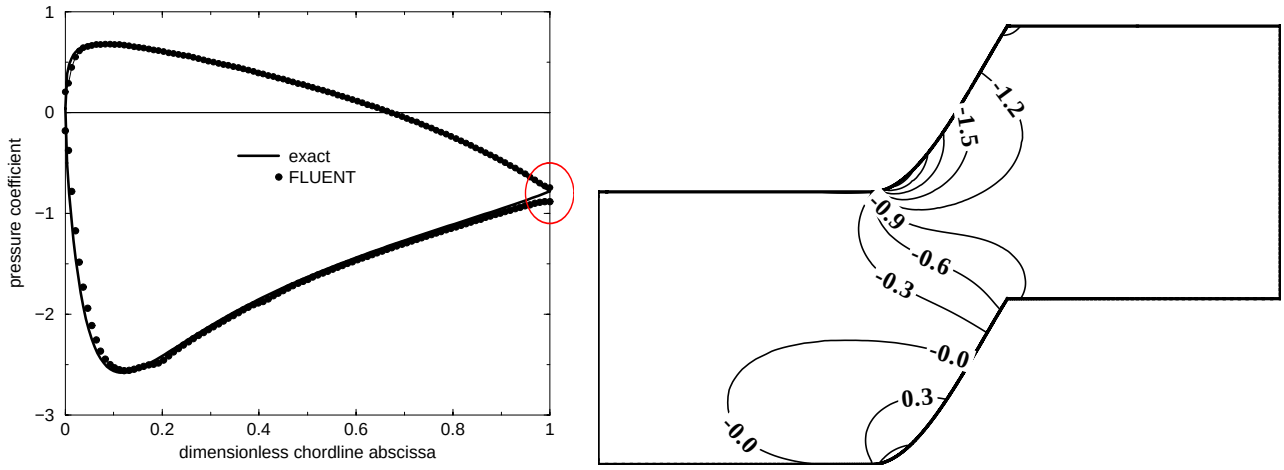

Figure 6. Pressure coefficient computed with FLUENT on the blade and in the inter-blade channel for a turbine cascade with $\alpha_1 = 35^\circ$ and $\alpha_2 = 55^\circ$ and $s/c = 1.270120$.

Going back to the absence of explicit Kutta-Joukowsky condition, we first see that there is a gap between the pressure on the suction/pressure sides at the trailing edge. It is interesting that the pressure on the pressure side matches almost perfectly the exact solution. However, on the suction side the numerical

values slightly depart from the exact solution close to the trailing edge. To elucidate this aspect, let us examine the total pressure field expressed by the total pressure coefficient defined similarly to the pressure coefficient (19),

$$c_{p_T} = \frac{p_T - p_{T1}}{\frac{1}{2}\rho \bar{V}_1^2}, \text{ where the total pressure is } p_T = p + \frac{1}{2}\rho V^2 . \tag{19}$$

According to the Bernoulli's theorem, c_{p_T} should vanish in the whole computational domain. However, as shown in Fig. 7 there is a total pressure defect on the foil suction side, as well as in an artificial wake downstream the hydrofoil. This is the implicit effect of the numerical viscosity embedded in the Euler solver, and it is not explicitly specified or controlled in the problem setup. Obviously, this numerical diffusion depends on the finite volume discretization scheme, as well as on the mesh refinement, but nevertheless it helps getting the almost correct velocity and pressure fields for the cascade flow. This feature of the Euler solvers is implicitly used also in more complex three-dimensional inviscid flow simulation in turbomachines, with surprisingly good results. The correct approach, however, is to consider the viscous turbulent flow with the physical boundary layer development on solid surfaces instead of relying on a rather ad-hoc numerical dissipation embedded in a numerical scheme that solves an inviscid flow.

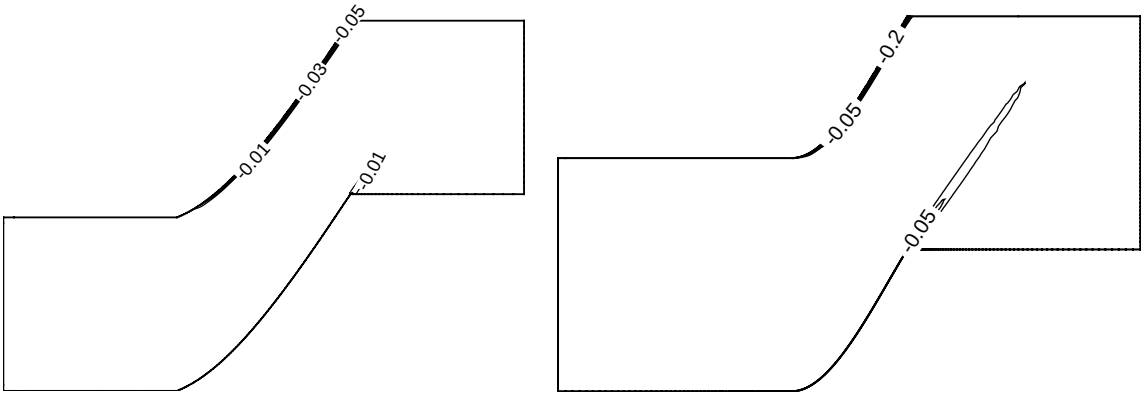

Figure 7. Total pressure deficit in spurious boundary layers and wakes for Euler flow simulation.

4. CONCLUSIONS

This paper presents the numerical analysis of thin hydrofoil cascades designed in the first part of the paper [15], using both Finite Element and Finite Volume methods.

First, the CASCADExpert finite element code developed by the authors is shown to produce accurate results for the pressure distribution on the blade, as well as for the streamline pattern. The original implementation of the Kutta-Joukovsky condition is validated for the difficult test case of thin hydrofoils. Second, the FLUENT finite volume code is used for solving the inviscid cascade flow in velocity/pressure formulation. It is shown that in this case the Kutta-Joukovsky condition is replaced by the numerical viscosity embedded in the numerical scheme used to discretize the Euler equations.

Both numerical methods confirm the shock-free flow at leading edge, and predict the correct flow deflection, or the outflow angle. The numerical analysis approaches developed and validated in this paper are going to be included in a complex cascade optimization methodology.

REFERENCES

1. BALAY, S., BUSCHELMAN, K., EIJKHOUT, V., GROPP, W., KAUSHIK, D., KNEPLEY, M., CURFMAN McINNES, L., SMITH, B., ZHANG, H., *PETSc Users Manual*, Argonne National Laboratory, ANL-95/11, Revision 2.2.1, 2004.
2. BALINT, D., SUSAN-RESIGA, R., *Numerical investigation of a NACA65 series low speed compressor cascade*, Buletinul Ştiinţific al Univ. Politehnica Timişoara, Seria Mecanică, Tom **45(59)**, pp. 7-14, 2000.
3. CARTE, I.N., *Contribuţii la studiul reţelelor de profile radial-axiale şi utilizarea lor în proiectarea rotorilor de turbine Francis*, Teza de doctorat, Institutul Politehnic "Traian Vuia" Timişoara, 1986.
4. CHANG, I.-C., TORRES, F.J., TUNG, C., *Geometric Analysis of Wing Sections*, NASA Technical Memorandum 110346, 1995.
5. FRUNZĂ, T., SUSAN-RESIGA, R., *Software Development for Cascade Flow Simulation*, in Proceedings of the Workshop on Numerical Simulation for Fluid Mechanics and Magnetic Liquids, Timişoara, Ed. Orizonturi Universitare, pp. 57-58, 2001.
6. FRUNZĂ, T., SUSAN-RESIGA, R., *Finite Element Analysis of Cascade Flows*, in Proceedings of the "Classics and Fashion in Fluid Machinery" Conference, Beograd, pp. 179-186, 2002.
7. FRUNZĂ, T., SUSAN-RESIGA, R., *Superconvergent Patch Recovery for Velocity Computation on Unstructured Mesh and Cascade Flow Application*, Proceedings of the Workshop on Numerical Methods in Fluid Mechanics and FLUENT Applications, Timişoara, Ed. Orizonturi Universitare, pp. 64-75, 2003.
8. HAWTHORNE, W.R., WANG, C., TAN, C.S., McCUNE, J.E., *Theory of Blade Design for Large Deflections: Part I – Two-Dimensional Cascade*, Journal of Engineering for Gas Turbines and Power, **106**, pp. 346-353, 1984.
9. HUGHES, J.R., The Finite *Element Method. Linear static and dynamic Finite Element Analysis*, Mineola, New York, Dover Publications, 2000 (reprint of *The Finite Element Method*, originally published by Prentice-Hall, 1987).
10. McFARLAND, E.R., *A Rapid Blade-to-Blade Solution for Use in Turbomachinery Design*, Journal of Engineering for Gas Turbines and Power, **106**, pp. 377-382, 1984.
11. MILNE-THOMSON, L.M., *Theoretical Hydrodynamics*, The MacMillan Press, 5th edition, 1968.
12. SUSAN-RESIGA, R., MUNTEAN, S., *Periodic Boundary Conditions Implementation for the Finite Element Analysis of the Cascade Flow*, Buletinul Ştiinţific al Univ. Politehnica Timişoara, Seria Mecanică, Tom **44**(**58**), pp. 151-160, 1999.
13. SUSAN-RESIGA, R., MUNTEAN, S., ANTON, I., *Numerical Analysis of Cascade Flow. Part I: Finite Element Analysis of the Inviscid Flow*, Buletinul Ştiinţific al Univ. Politehnica Timişoara, Seria Mecanică, Tom **45**(**59**), pp.159-166, 2000.
14. SUSAN-RESIGA, R., *Mecanica Fluidelor Numerică*, Timişoara, Ed. Orizonturi Universitare, 2003.
15. SUSAN-RESIGA, R., MUNTEAN, S., BERNAD, S., FRUNZĂ, T., BALINT, D., *Thin Hydrofoil Cascade Design and Numerical Flow Analysis. Part I – Design*, Proceedings of the Romanian Academy, Series A: Mathematics, Physics, Technical Sciences, Information Science, (to appear)
16. ***, FLUENT 6 User's Guide, 2001.

Received January 12, 2006